International Journal of Bifurcation and Chaos, Vol. 9, No. 4 (1999) 745–756

FEEDBACK LOOP IN EXTENDED VAN DER POL'S EQUATION APPLIED TO AN ECONOMIC MODEL OF CYCLES*

SAFIEDDINE BOUALI†
University of Tunis III, Management Institute, Department of Economics, 41, rue de la Liberté, 2000 Le Bardo, Tunisia

Received October 15, 1997; Revised August 1, 1998

We connect to the Van der Pol's equation an appropriate feedback loop which unfolds a wide range of dynamic behavior. The bifurcation diagrams reveal the rise, then the extinction of the chaos bubble. Moreover, the numerical computations display an antisymmetric strange attractor with morphological plasticity by the variation of the sole feedback control parameter. This chaotic 3D system is built to found an heuristic model of economic cycles focused on the capital flight observed in the less developed countries. The model exhibits the ability of the potential GDP to drive the growth dynamic.

1. Introduction

The equation of Van der Pol [1926] constitutes an eminent model to analyze the dynamic behavior of (self) excited oscillations. Several authors have well studied the outcome of a *T-periodic* forcing function [Parlitz & Lauterborn, 1987] and a scalar bias [Thompson & Stewart, 1988] in the Van der Pol's equation (VdPe).

In this paper, we investigate the next step of this methodology. Indeed, we study the outcome of a retroactive loop determined by the state variables of VdPe itself. This connection establishes a full feedback linkage and allows homoclinicity which may lead to a route to chaos [Nicolis, 1995; Lakschmanan & Murali, 1996]. One would expect a similar behavior in our application.

In Sec. 2, we study numerically the behavior of the (electrical) VdPe connected with a particular feedback circuit and its dynamical characteristics. We determine (1) the bifurcation diagrams by varying the control parameter of the feedback in order to detect its global effect; then, we identify (2) the chaotic attractors and their nature. The new system lays the foundation of heuristic modelization of economic cycles (Sec. 3) by the relevance of the saving behavior to the potential Gross Domestic Product in the Less Developed Countries (LDC). Hence, in Sec. 4, we indicate the piecewise curve of the "physical" model and the findings of our economic model to the development policy.

2. The Model

Written in two first-order ordinary differential equations, the VdPe is connected to a feedback function (z-equation) controlled by a parameter s. It is assumed that the additional (linear) ordinary differential equation which represents the perturbation founds a new 3D system. The set of the three first-order coupled equations (k, μ, b, s, p and q: positive parameters):

$$\frac{dx}{dt} = ky + \mu x(b - y^2) \qquad (1)$$

*I am grateful to the anonymous referees to their suggestions and comments. Remaining errors are ours.
†E-mail: Safieddine.Bouali@isg.rnu.tn

$$\frac{dy}{dt} = -x + sz \tag{2}$$

$$\frac{dz}{dt} = px - qy \tag{3}$$

defines stationary equilibria obtained for $dx/dt = dy/dt = dz/dt = 0$.

We get $z = x/s$ from Eq. (2), $y = x(p/q)$ from Eq. (3) and $x = ky/\mu(y^2 - b)$ from Eq. (1).

The last two equalities yielded the following polynomial relation: $x^3(p/q)^2\mu - (\mu b + k(p/q))x = 0$.

The three roots are: $x_1 = 0$, $x_2 = [\mu b + k(p/q)]/[(p/q)^2\mu]^{1/2}$ and $x_3 = -[\mu b + k(p/q)]/[(p/q)^2\mu]^{1/2}$.

Let $[\mu b + k(p/q)]/[(p/q)^2\mu]^{1/2} = \alpha$, the three equilibria become: $E_1(x, y, z) = (0, 0, 0)$, $E_2(x, y, z) = (\alpha, (p/q) \cdot \alpha, (1/s) \cdot \alpha)$ and $E_3(x, y, z) = (-\alpha, -(p/q) \cdot \alpha, -(1/s) \cdot \alpha)$.

E_2 and E_3 are antisymmetric.

On the other hand, the Jacobian matrix is:

$$J(x, y, z) = \begin{bmatrix} \mu(b - y^2) & k + 2\mu xy & 0 \\ -1 & 0 & s \\ p & -q & 0 \end{bmatrix}.$$

Hence, we obtain $|J| = sp(k + 2\mu xy) + sq\mu(b - y^2)$

For a particular specification P_0: $(k, \mu, b, p, q) = (0.02, 0.4, 0.2, 10, 0.1)$, E_1 is unstable since $|J| = (pk + q\mu b)s = 0.208s > 0$, for any (positive) value of control parameter s.

The two other equilibria, for instance at $s = 0.2$, $E_2 = (0.02, 2.28, 0.11)$ and $E_3 = -E_2$ are also unstable since $|J| = 0.105 > 0$.

The total number of diagonal items of J matrix is $\mathrm{Tr}(J) = 0.4\ (0.2 - y^2)$ which shows that the model is conservative for the trajectories that are close to the solutions E_1, E_2 and E_3, but the flow is dissipative for the peripheral orbits ($|y| > 0.447$). For this last case, the contraction of the volume is equal to $\exp[0.4(0.2 - y^2)]$ by time unit.

To identify the feedback outcome, the numerical computations are carried out with the fifth-order Runge–Kutta integration method and accuracy (or the unit of time) equal to 10^{-5}. All simulations are started with initial conditions: $(x, y, z) = (0, 0.01, 0)$ and the specification of parameters P_0.

2.1. *Global bifurcations, blue sky catastrophe and chaotic behavior*

For very low values of control parameter s, the dynamic of the z-variable remains similar to the case of nonconnection to the VdPe (Fig. 1). Until $s \simeq 5.10^{-5}$, the bifurcation diagrams of the variables show the persistence of the VdPe limit-cycle (Fig. 2). Beyond $s \simeq 10^{-4}$, z-variable follows a different trajectory and dives both the variables x and y into an unstable zone. As for variable x, it is projected towards the origin, while y is rejected to a zone that is outside the limit-cycle.

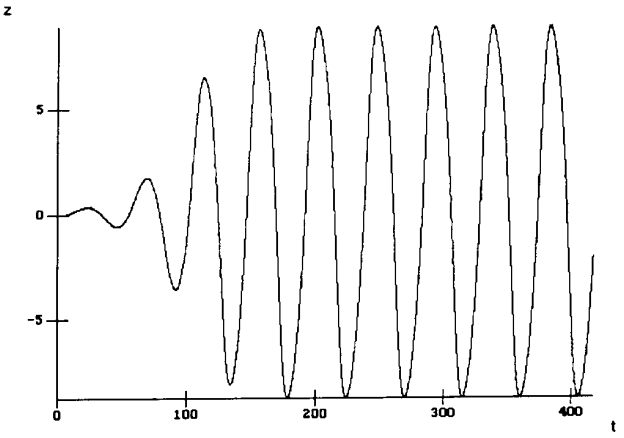

Fig. 1. Behavior of the feedback ($s = 0$). The z-variable emits a *period-2* signal in the case of nonconnection.

As s increases further, i.e. for the less weak amplification intensity of the feedback, a loss of stability of a *period-2* solution occurs in the homoclinic direction (z-axis) leading to stable and unstable dynamics (Fig. 3).

However, the "blue sky catastrophe" phenomenon occurs since the computed diagrams of y and z variables stop for $s \simeq 0.004$ and do not plot any more points. Yet, when $s \simeq 0.008$, the diagrams reoccur. Nevertheless, for a wider s step-size, this phenomenon is masked.

The VdPe limit-cycle is now supplanted by an utterly different trajectory associated with the homoclinic bifurcation (Fig. 4).

For very high amplifications of the feedback, the global bifurcation diagrams show a cascade of period-halving bifurcations to stability for all variables; afterwards a "stalling" phenomenon appears (Fig. 5). The feedback is no more turbulent and the model acquires an infinitely fixed structure represented by a stable *period-2* solution for $s \simeq 280$.

Nonetheless, the bifurcation diagrams are sensitive to s step-size. Indeed, with the step-size $s = 10^{-4}$ the obtained diagram takes a different orientation. The bifurcation towards a higher or lower branch stems up after an alternation of a

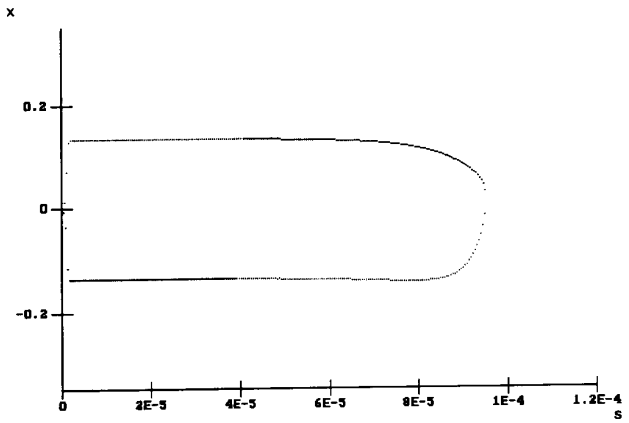

(a)

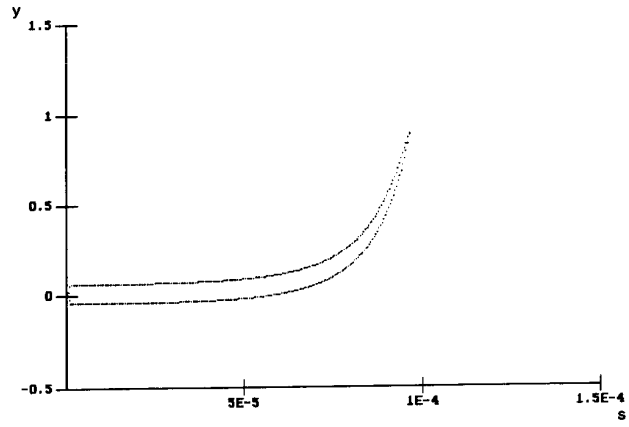

(b)

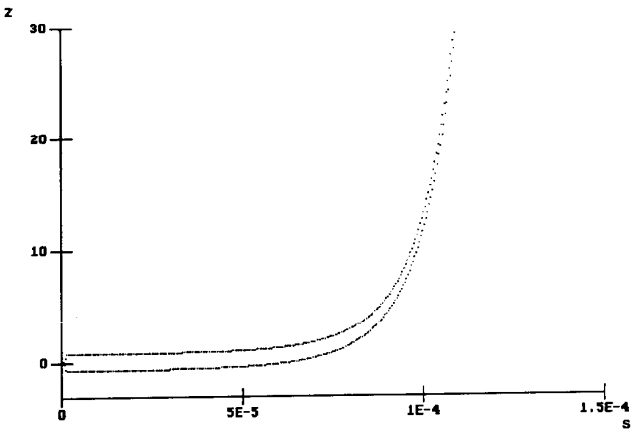

(c)

Fig. 2. Bifurcation diagrams for the Poincaré return map (s step-size = 10^{-8}). At very weak values of s, the limit-cycle of the state variables of VdPe remains stable, as well as the motion of the (internal) perturbation. At $s \simeq 6.10^{-5}$, (a) x-variable is projected to origin while (b) y-variable and (c) z-variable are thrown to high values.

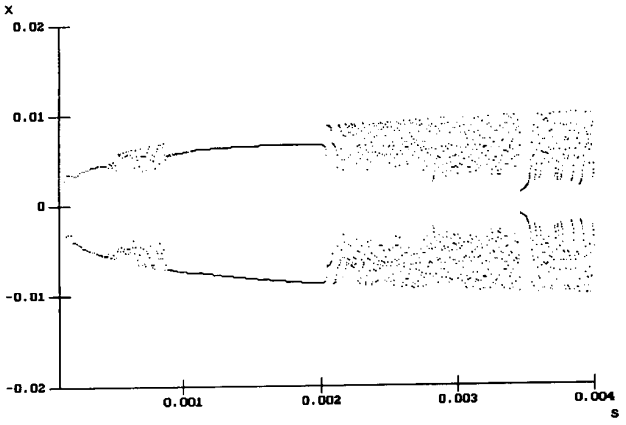

(a)

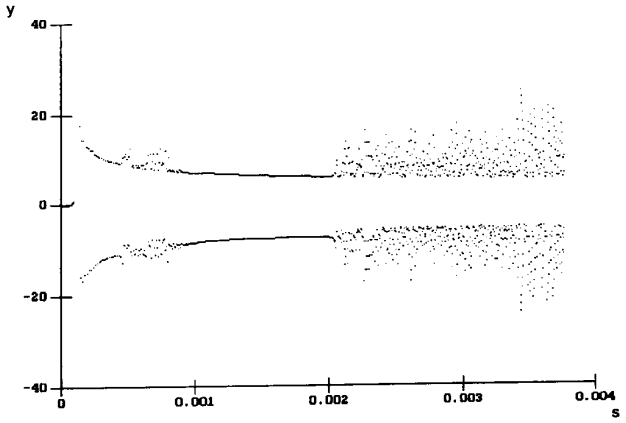

(b)

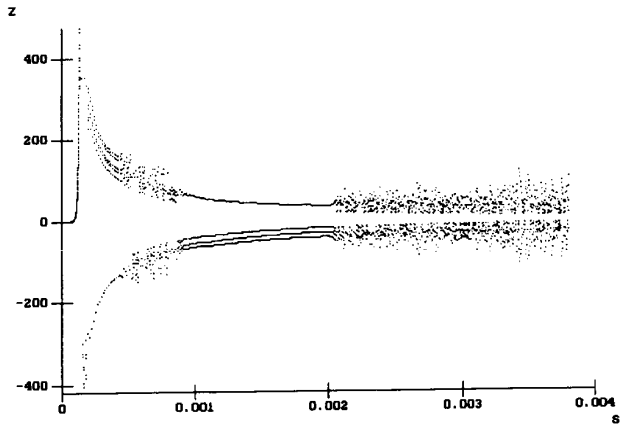

(c)

Fig. 3. Blue sky catastrophe. Periodic and chaotic dynamics occur for all variables. The ending of diagrams is observed only for y and z variables at $s \simeq 0.004$.

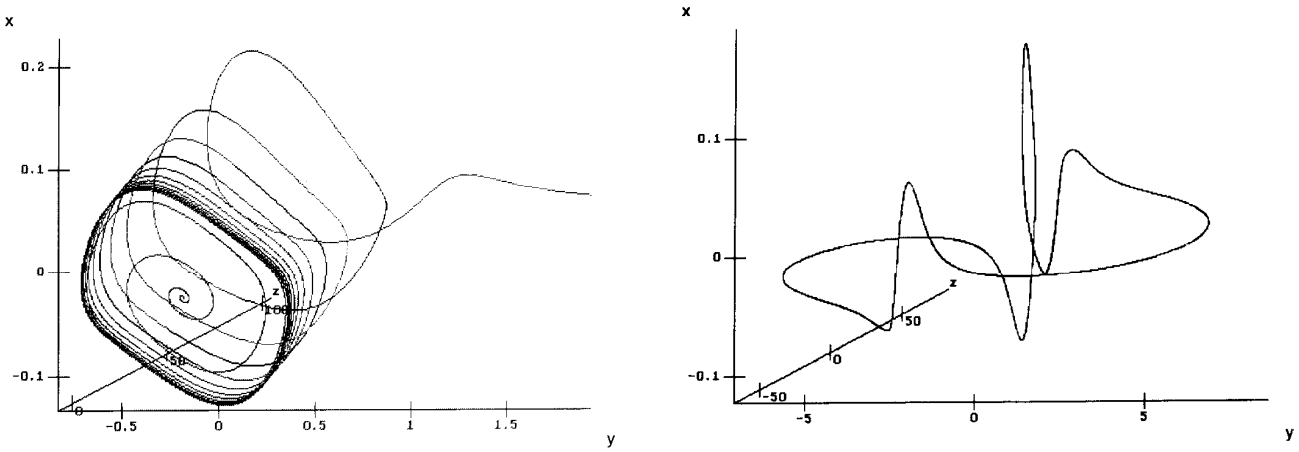

(a) (b)

Fig. 4. Homoclinic bifurcation. For $s = 10^{-3}$, (a) an homoclinic bifurcation appears and exhibits (b) periodic motion.

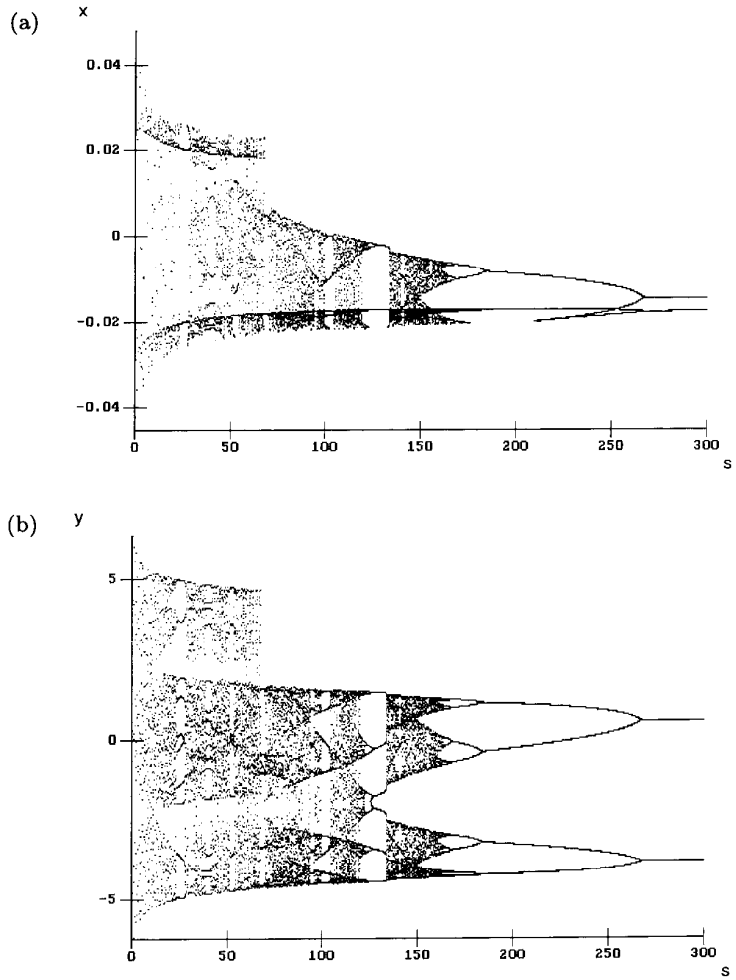

Fig. 5. Bifurcation diagrams for the Poincaré return map (s step-size $= 10^{-2}$). The feedback effect gives a chaotic bubble but extinguishes at final *period-2* solution for (a) x and (b) y state variables. The chaotic motion is observed also for (c) retroactive z-variable. We notice that the diagrams are not symmetric beyond $s \simeq 70$.

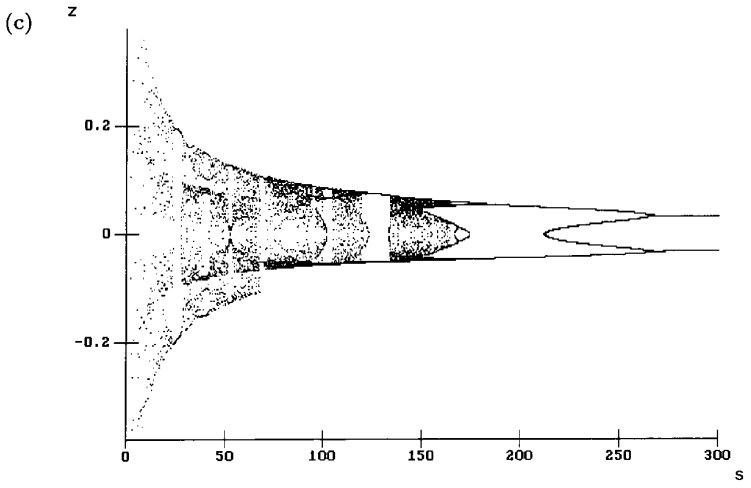

Fig. 5. (*Continued*)

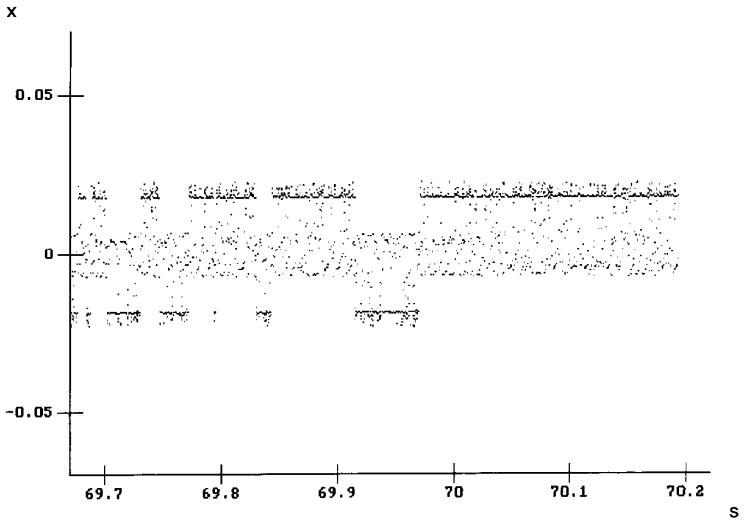

Fig. 6. Bifurcation trap. Simulation of bifurcation diagram of x started with s step-size $= 10^{-4}$. Beyond $s \simeq 70$, the bifurcation in high or low branch is determined by the step-size of control parameter s. This diagram of x shows a bifurcation trapping in a high sub-basin of attraction, while, in Fig. 5(a), it is trapped in the lower sub-basin with another step-size.

high–low sequence. The trajectories follow several orbits in the high sub-basin before taking the direction of the low sub-basin and vice-versa. The one ten-thousandth fraction of s is decisive for the bifurcation where these trajectories are eventually trapped (Fig. 6).

On the other hand, in the inside of stability windows, several stable *period-nT* order solutions occur whose phase space follows the cascade of period-doubling then period-halving bifurcations (Fig. 7).

2.2. *Chaotic attractors and the Lyapunov exponents*

With a particular value of s parameter, an antisymmetric chaotic attractor occurs (Fig. 8) and the variation of s is enough to produce another chaotic

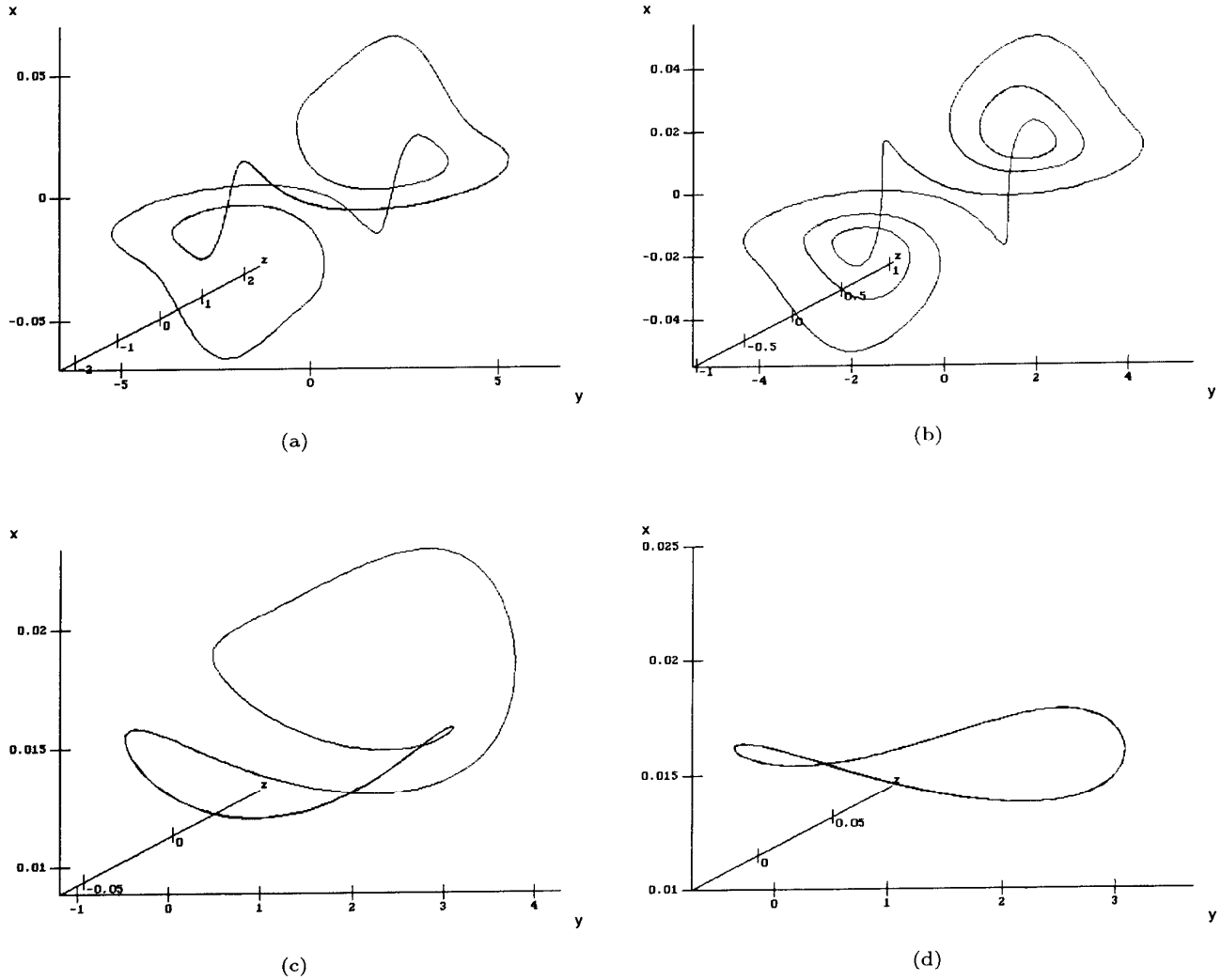

Fig. 7. Several periodical solutions. In the periodic windows of bifurcation diagrams, the period order increases then decreases according to s parameter. (a) *Period-6* solution for $s = 0.5$, (b) *period-10* solution at $s = 1.5$, (c) *period-4* solution for $s = 215$ and (d) *period-2* solution at $s = 280$.

attractor with a complex structure (Fig. 9). This symmetry inversion is created by the mechanism of [Silnikov, 1965].

Nevertheless, beyond $s \simeq 70$, the Sensitive Dependence on s Parameter (SDP) becomes specifically different as the chaotic attractors lose their antisymmetry. The basin of attraction is now split into two sub-basins that are distinct. Thus, the model produces two attractors (for only one s value) with an antisymmetric position (Fig. 10). Hence, the closure of a dynamic in a particular sub-basin is the result of Sensitive Dependence on Initial Conditions (SDIC). The Poincaré maps reflect this morphological plasticity — according to s — either for antisymmetric strange attractors or nonsymmetric ones (Fig. 11).

Simultaneously, the SDIC and SDP induce the presence of "strange" characteristics [Medio, 1993] of these chaotic attractors. Besides, for $s = 35$, the Lyapunov Characteristic Exponents are positive: LCE $(x, y, z) = (0.27, 0.65, 0.41)$.

We derive from this chaotic 3D system a model of economic cycle suited for heuristic approach.

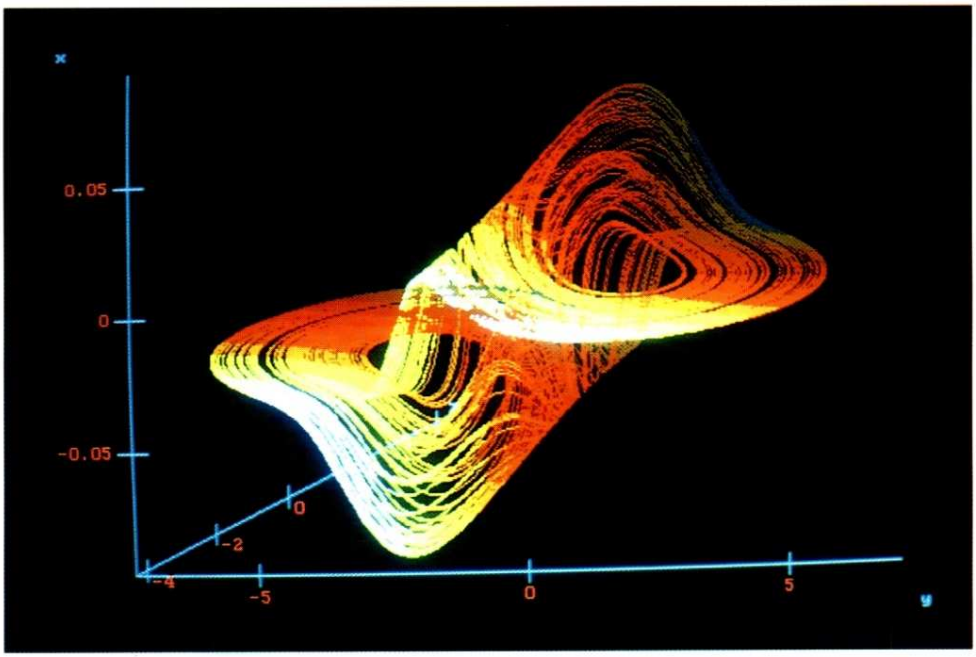

Fig. 8. Strange attractor. A strange attractor occurs with two homoclinic orbits for $s = 0.2$.

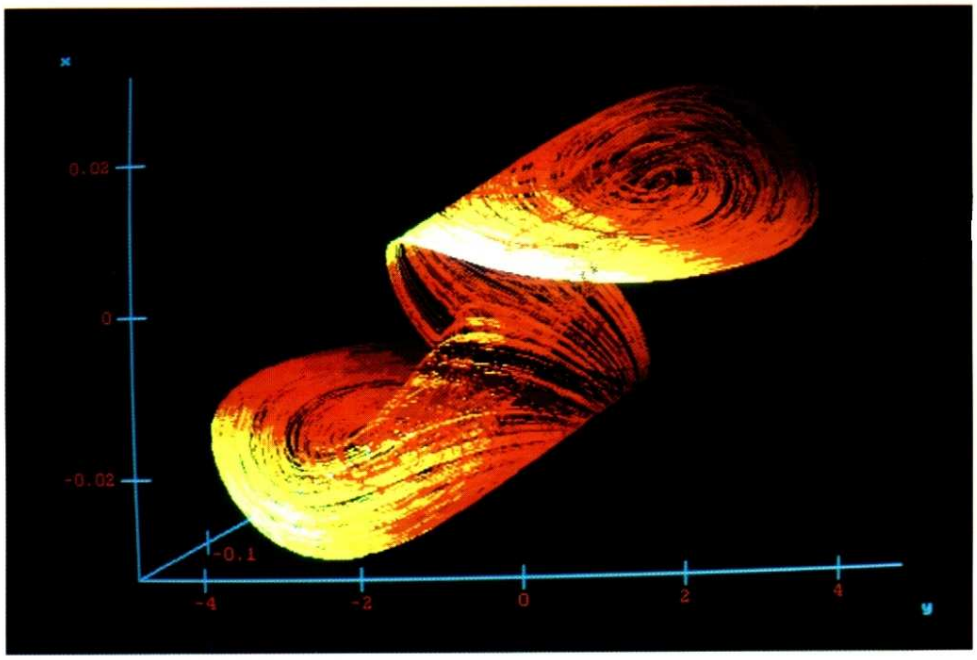

(a)

Fig. 9. Complexity of strange attractor. A strange attractor, for $s = 35$, displayed in three different Euclidian coordinate representations.

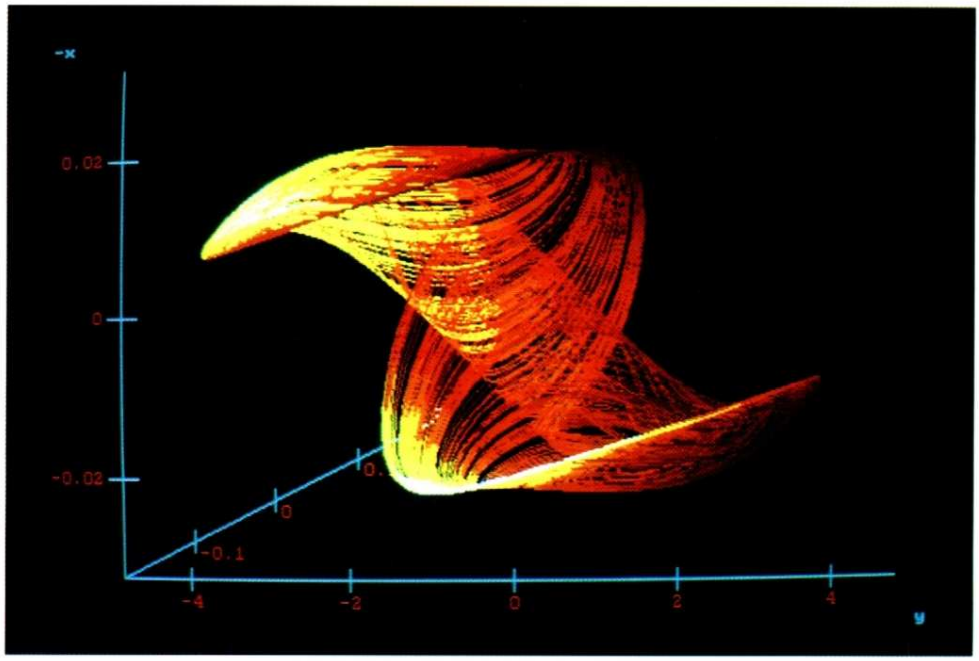

(b)

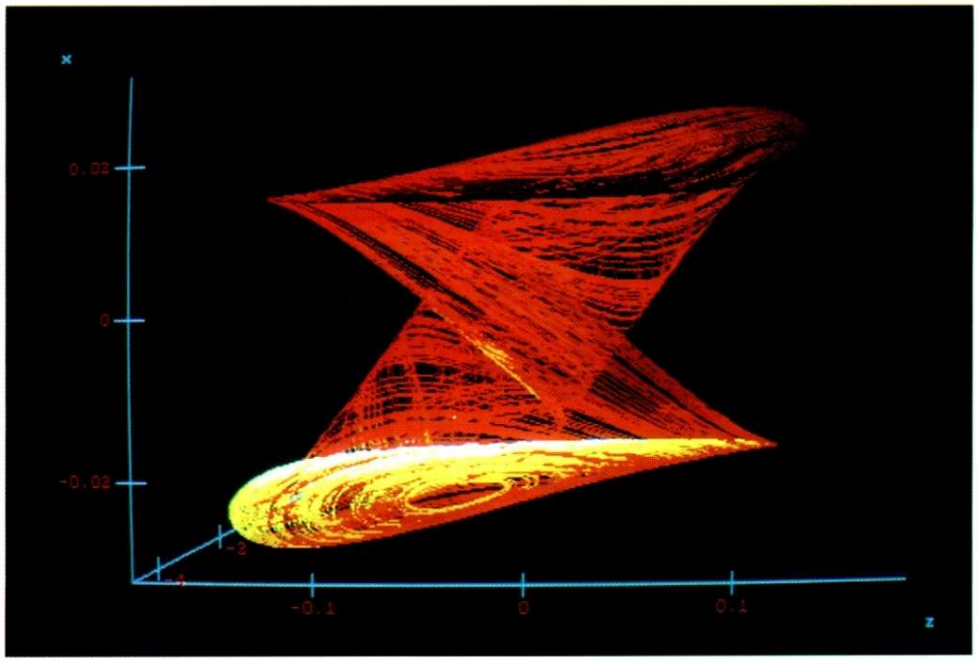

(c)

Fig. 9. (*Continued*)

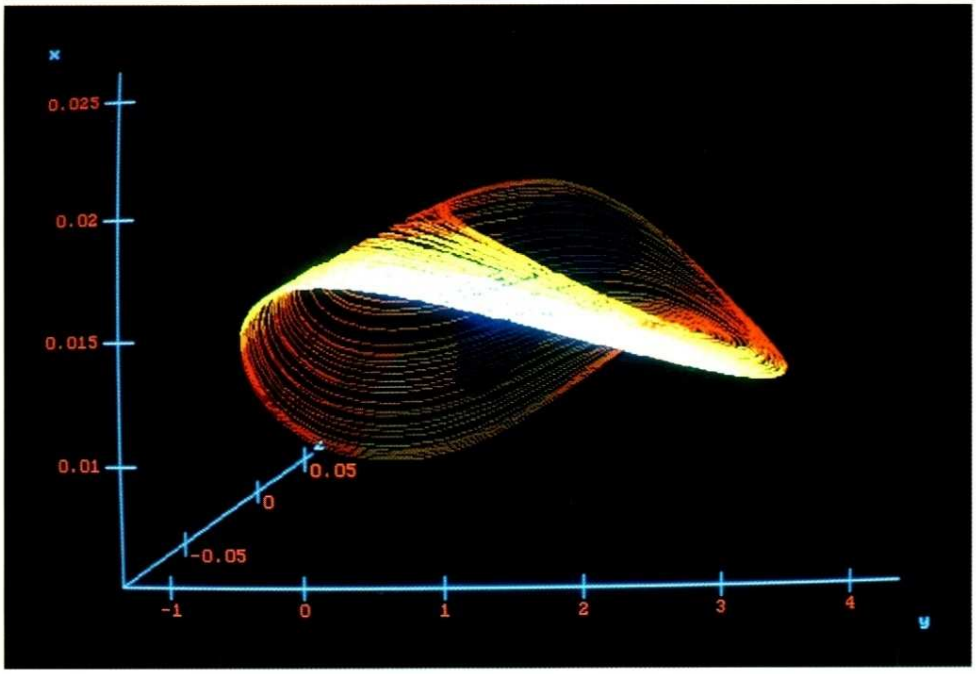

(a)

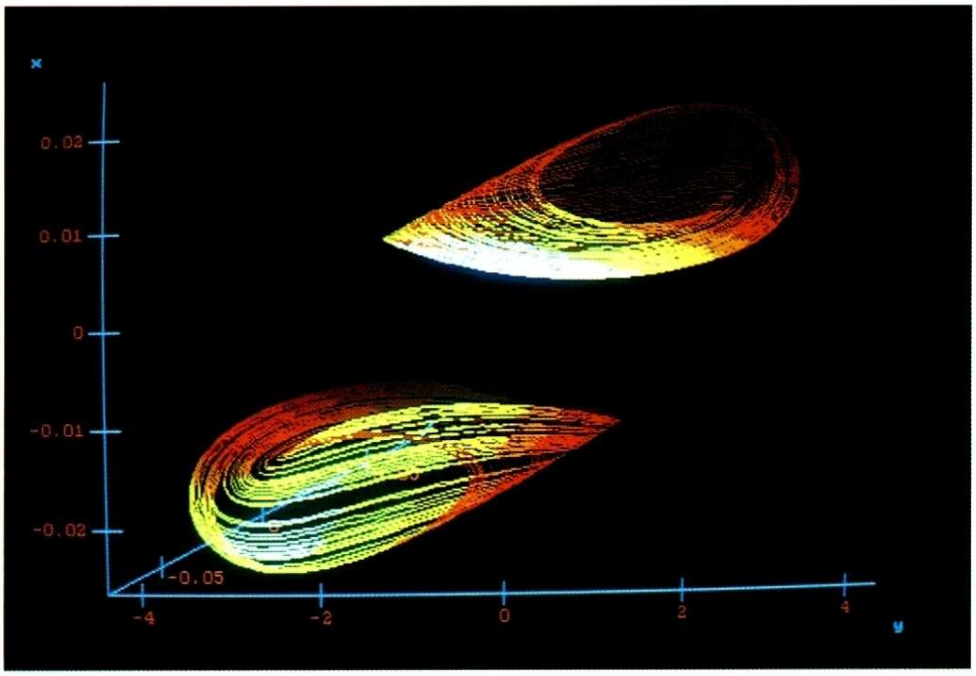

(b)

Fig. 10. Strange attractors without antisymmetric structure. For $s = 150$, (a) the strange attractors lose the antisymmetry structure (no-bridge between the high and low sub-basins). Thus, (b) each sub-basin produces a strange attractor.

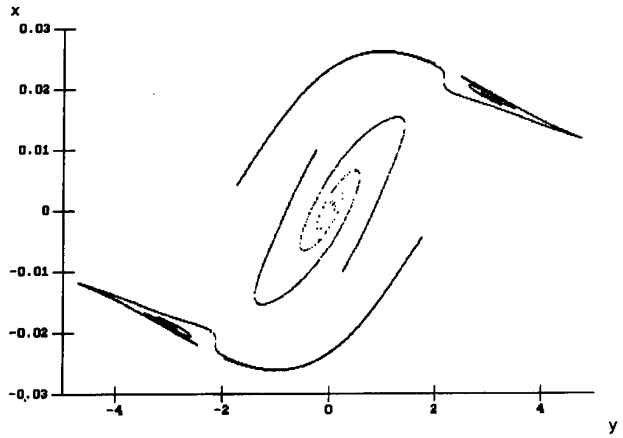

(a)

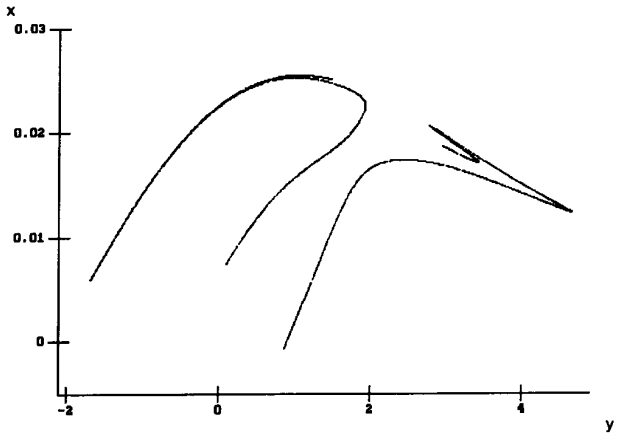

(b)

Fig. 11. Poincaré maps. The map is antisymmetric before $s \simeq 70$, for example (a) $s = 58$ and nonsymmetric after this threshold, for instance (b) $s = 73$. In the last case, the model gives two Poincaré maps for each s value by antisymmetric initial conditions.

3. The Economic Model of Cycles

We introduce briefly an economic model of cycles focused on the capital flight phenomenon observed in the LDC [Cuddington, 1986]. To build the model, we keep unchanged the Eqs. (1) and (3) written with economic symbols.

The saving equation is:

$$\frac{dS}{dt} = aY + p(Y^* - Y^2)S \qquad (1.1)$$

where S stands for Saving (households), Y for Gross Domestic Product (GDP) and Y^* represents the value of potential GDP (scalar). On the other hand, a is the variation of the marginal propensity to saving while p is the ratio of capitalized profit.

According to the life cycle hypothesis [Ando & Modigliani, 1963; Modigliani, 1988], the households will continuously increase the marginal propensity to saving. The quick extension of life expectancy [Cutler *et al.*, 1990] and the weak expansion of the social security [Kimball, 1990] both in LDC reinforce this tendency.

The potential value of GDP [Okun, 1962] is measured by a full employment of the industrial capacities. In this application, Y^* demarcates the upward side from the downward one of the capitalized profits. For the LDC, the industry creation is locked in the traditional comparative advantages. If $Y < Y^*$, there will be a sharp increase of profit since the activities are not constrained by the plants. They derive high profits since these sectors have been just started and their markets are not yet saturated. When the profits are shared, they will be re-injected into the financing circuit. The nonlinear specification indicates the braking of profit withdrawal outside the productive system thereby driving a better capitalization.

On the contrary, at the neighborhood and beyond Y^* the threat of inflation appears. Not only are the shared profits not reinvested, but also the households will deviate their capital due to the lack of new investment opportunities. The saving deviation is accelerated in relation with the gap between the GDP and its potential value.

Besides, the equation of GDP takes the form:

$$\frac{dY}{dt} = \frac{(S+F)}{v} \qquad (2.1)$$

where F is the foreign capital inflow (net) and v the capital–output ratio.

The capital constitutes the fundamental constraint in the development process. Hence, the GDP is determined by the level of investments. They are financed by the household's saving and by the foreign capital inflows.

On the other hand, the equation of foreign financing is:

$$\frac{dF}{dt} = mS - rY\,, \qquad (3.1)$$

m stands for capital inflow-saving ratio and r for debt refund–output ratio.

The capital inflows constitute a complement of the saving and the capital refund is a constant proportion of output level. This relation is a simplified

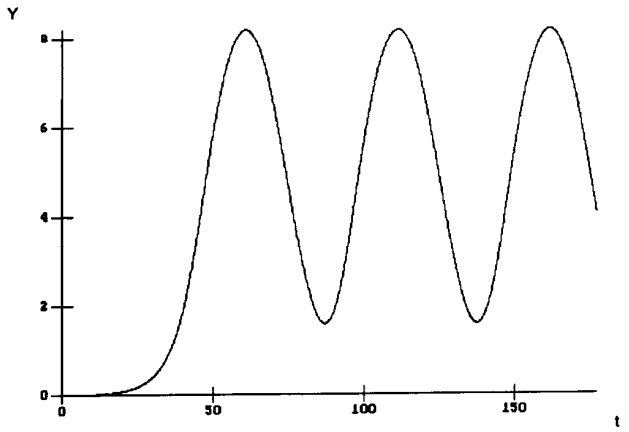

(a)

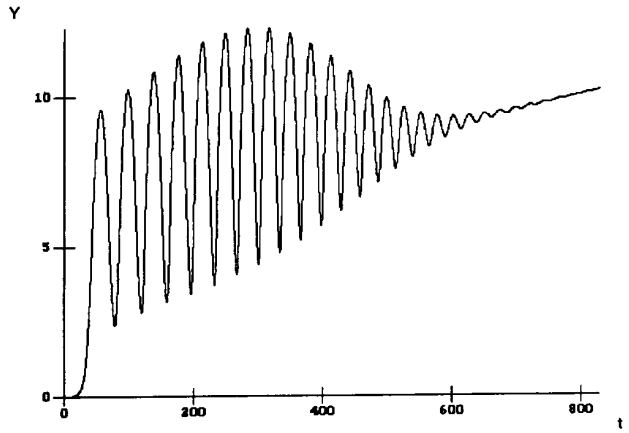

(b)

Fig. 12. The behavior of the economic cycle. (a) When Y^* is fixed, the dynamic of GDP converges to a stationary cycle for particular initial conditions. (b) If the potential GDP grows with a constant rate ($n = 0.1$) then, the fluctuations of GDP are damped and substituted by a sustainable growth.

account of the international financial movements of LDC.

Eventually, the path of the potential GDP:

$$\frac{dY^*}{dt} = n\,, \tag{4}$$

n: is rate of growth.

In our application, we shall specify values selected from several LDC [Summers & Heston, 1991]. Indeed, the specification of parameters is C: $(a, p, v, m, r) = (0.04, 0.02, 4, 0.3, 0.03)$ but the potential GDP shall have the arbitrary initial value $Y^* = 1$. Our analysis shall deal with the influence of the potential GDP (n: control parameter) on the economic stability.

When Y^* is unchanging ($n = 0$), the dynamic of GDP is a semi-attractor [Fig. 12(a)]. However, if $n > 0$, the stationary cycle or the stagnation of the GDP could be converted to sustained growth [Fig. 12(b)]. Moreover, the fluctuations are more damped if n increases.

Even though, the observed potential GDP series of wide number of LDC alternates sequences of stagnation and growth, our application highlights a significant stylized fact. Without technological progress of the key-sectors, the households divert their savings from the productive system. The potential GDP inertia hinders the continuous capitalization of profits and the investments are deprived from substantial financial flows, since the saturation of traditional activities constitutes a motive of capital flight. The comparative advantage framework based on labor costs is exhausted in the development process. The R&D programs and the sustainable industrial expansion in modern sectors drive the turning points of the saving cycle, allow the maintenance of the capitalization of profits and neutralize the capital flight.

4. Antiequilibrium Feedback

The chaotic 3D system, studied in Sec. 2, leads the flows around three unstable equilibria. Indeed, the piecewise curve is nonlinear knowing that the absolute value of the slope at the neighboring of equilibria must be smaller than 1 to report their instability (Fig. 13). The methodology of antiequilibrium excitation in the extended VdPe, shows the power of a feedback loop leading to a wide range of dynamics. The particular feedback does not release an infinite chaotic expansion (except for the limit case of "blue sky catastrophe"). Even, if the chaotic bubble is restricted in a finite interval of s, it does not mean that the effect of feedback is transitory since the final *period-2* dynamic is different from the generic VdPe limit-cycle. We investigate the range of its dynamic solutions and modify a single equation to lay open to heuristic modelization of economic cycles. Connecting a similar feedback loop in a stationary version of the VdPe, the model of cyclical growth also provides homoclinicity leading to chaotic behavior. However, with specific values from LDC, the application displays the required promotion

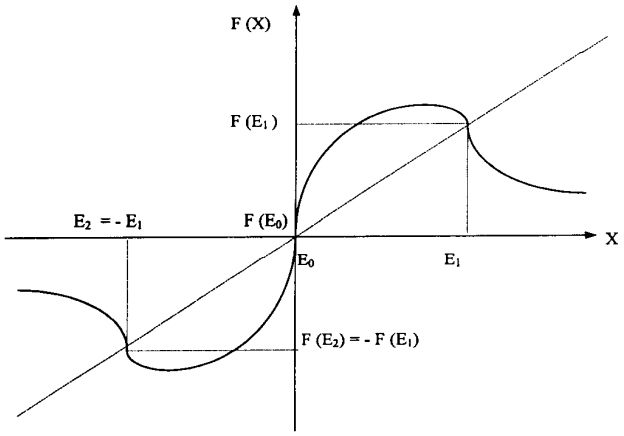

Fig. 13. Characteristic curve. The "physical" model leads the flows around three unstable equilibria. The curve is nonlinear according to Eq. (1). Beyond $s \simeq 70$, it is split in two separable functions.

of new industrial frameworks in the development process.

References

Ando, L. & Modigliani, F. [1963] "The 'life cycle' hypothesis of saving: Aggregate implications and test," *Am. Econ. Rev.* **53**, 55–84.

Cuddington, J. T. [1986] "Capital flight: Estimates, issues and explanations," *Princeton Studies in Int. Finance* **58**.

Cutler, D. M., Potera, J. M., Sheiner, L. M. & Summers, L. H. [1990] "An aging society: Opportunity or challenge?" *Brooking Papers on Economic Activity* **21**, pp. 1–73.

Kimball, M. S. [1990] "Precautionary saving and the marginal propensity to consume," *NBER Working Paper* **3403**.

Lakshmanan, M. & Murali, K. [1996] *Chaos in Nonlinear Oscillators. Controling and Synchronisation*, World Scientific Series on Nonlinear Science, Vol. A(13), ed. Chua, L. O. (World Scientific, Singapore).

Medio, A. [1993] *Chaotic Dynamics, Theory and Applications to Economics* (Cambridge University Press).

Modigliani, F. [1988] "The role of intergenerational transfers and life cycle saving in the accumulation of wealth," *J. Econ. Perspectives* **2**, 15–40.

Nicolis, G. [1995] *Introduction to Nonlinear Science* (Cambridge University Press, Cambridge).

Okun, A. [1962] *Potential GNP: Its Measurement and Significance*; Reprint in Okun, A. [1970] *The Political Economy of Prosperity* (The Brooking Institution, Washington D.C.), pp. 132–145.

Parlitz, U. & Lauterborn, W. [1987] "Period-doubling cascades and devil's staircases of the driven Van der Pol oscillator," *Phys. Rev.* **A36**(3), 1428–1434.

Silnikov, L. P. [1965] "A case of the existence of a denumbrable set of periodic motion," *Sov. Math. Dokl.* **6**, 163–171.

Summers, R. & Heston, A. [1991] "The Penn world tables (Mark 5): An expanded set of international comparisons," 1950–1988," *Quart. J. Econ.* **106**(2), 327–368.

Thompson, J. M. T. & Stewart, H. B. [1988] *Nonlinear Dynamics and Chaos* (John Wiley, NY).

Van der Pol, B. [1926] "On relaxation oscillations," *Philos. Mag.* **7**(2), 978–992.